NANO LETTERS

Letter

pubs.acs.org/NanoLett

Controlling Random Lasing with Three-Dimensional Plasmonic Nanorod Metamaterials

Zhuoxian Wang,[†] Xiangeng Meng,*[,†] Seung Ho Choi,[‡] Sebastian Knitter,[§] Young L. Kim,[‡] Hui Cao,[§] Vladimir M. Shalaev,[†] and Alexandra Boltasseva*[,†]

[†]School of Electrical and Computer Engineering and Birck Nanotechnology Center, Purdue University, 1205 West State Street, West Lafayette, Indiana 47907, United States

[‡]Weldon School of Biomedical Engineering, Purdue University, 206 S. Martin Jischke Drive, West Lafayette, Indiana 47907, United States

[§]Department of Applied Physics, Yale University, New Haven, Connecticut 06250, United States

Supporting Information

ABSTRACT: Plasmonics has brought revolutionary advances to laser science by enabling deeply subwavelength nanolasers through surface plasmon amplification. However, the impact of plasmonics on other promising laser systems has so far remained elusive. Here, we present a class of random lasers enabled by three-dimensional plasmonic nanorod metamaterials. While dense metallic nanostructures are usually detrimental to laser performance due to absorption losses, here the lasing threshold keeps decreasing as the volume fraction of metal is increased up to ∼0.07. This is ∼460 times higher than the optimal volume fraction reported thus far. The laser supports spatially confined lasing modes and allows for efficient modulation of spectral profiles by simply tuning the polarization of the pump light. Full-field speckle-free imaging at micron-scales has been achieved by using plasmonic random lasers as the illumination sources. Our findings show that plasmonic metamaterials hold potential to enable intriguing coherent optical sources.

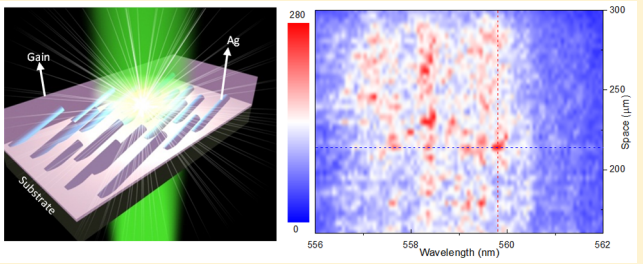

KEYWORDS: *Random lasers, plasmonics, metamaterials, lasing mode confinement, imaging*

Random lasers (RLs), optical sources that achieve feedback through multiple scattering of light, have attracted much attention in recent years owing to their unique properties.[1−6] In addition to a broad range of fundamental interests, RLs have also brought new opportunities in the fields of light-emitting diodes,[7] biological probes,[8] and optical imaging.[9] Recently, there has been a growing research interest in the effective control of random lasing properties such as directionality,[10] mode-locking transition,[11] and mode switching.[12] As a potential solution to these desires, the emerging field of nanoplasmonics, or photonics with metallic nanostructures, offers unique opportunities to control RLs.[13−20] This is related to the fascinating optical properties exhibited by metallic nanostructures that go beyond their dielectric counterparts; namely, the strong scattering capability, tunable scattering profile, and the existence of so-called plasmonic "hot spots".[21−23] Consequently, intense optical feedback for random lasing is anticipated at selective frequencies when metallic nanostructures are introduced to provide optical feedback for lasing. Additionally, the optical responses (e.g., absorption, scattering, near-field enhancement) of metallic nanostructures with anisotropic morphologies are highly sensitive to the polarization of incident waves,[24] which can enable tunable RLs with anisotropic plasmonic resonances. However, there is a bottleneck that hinders further development of such RLs. On one hand, densely packed metallic nanostructures are preferable to enable profound fluorophore−metal interactions and highly effective RLs. On the other hand, the presence of dense metallic components is usually thought to be detrimental to random lasing due to the high absorption losses.[13,25] Furthermore, the complete randomness of metallic nanostructures (e.g., positions and orientations) arising from traditional fabrication processes of RLs restrains the controllability by the plasmonic resonances.[13−18] Consequently, there is a need for the development of new techniques to overcome the aforementioned issues and eventually to control random lasing oscillations as desired.

In this work, we introduce an approach based on plasmonic metamaterials, structures that are artificially engineered to function beyond naturally occurring materials,[26−29] to reach a regime of unique random lasing oscillations. The plasmonic metamaterial is composed of three-dimensional (3D), densely packed, and tilted silver nanorods (NRs) that have a well-defined orientation to provide the optical feedback required for

Received: January 4, 2016
Revised: March 22, 2016
Published: March 29, 2016

DOI: 10.1021/acs.nanolett.6b00034
Nano Lett. 2016, 16, 2471−2477

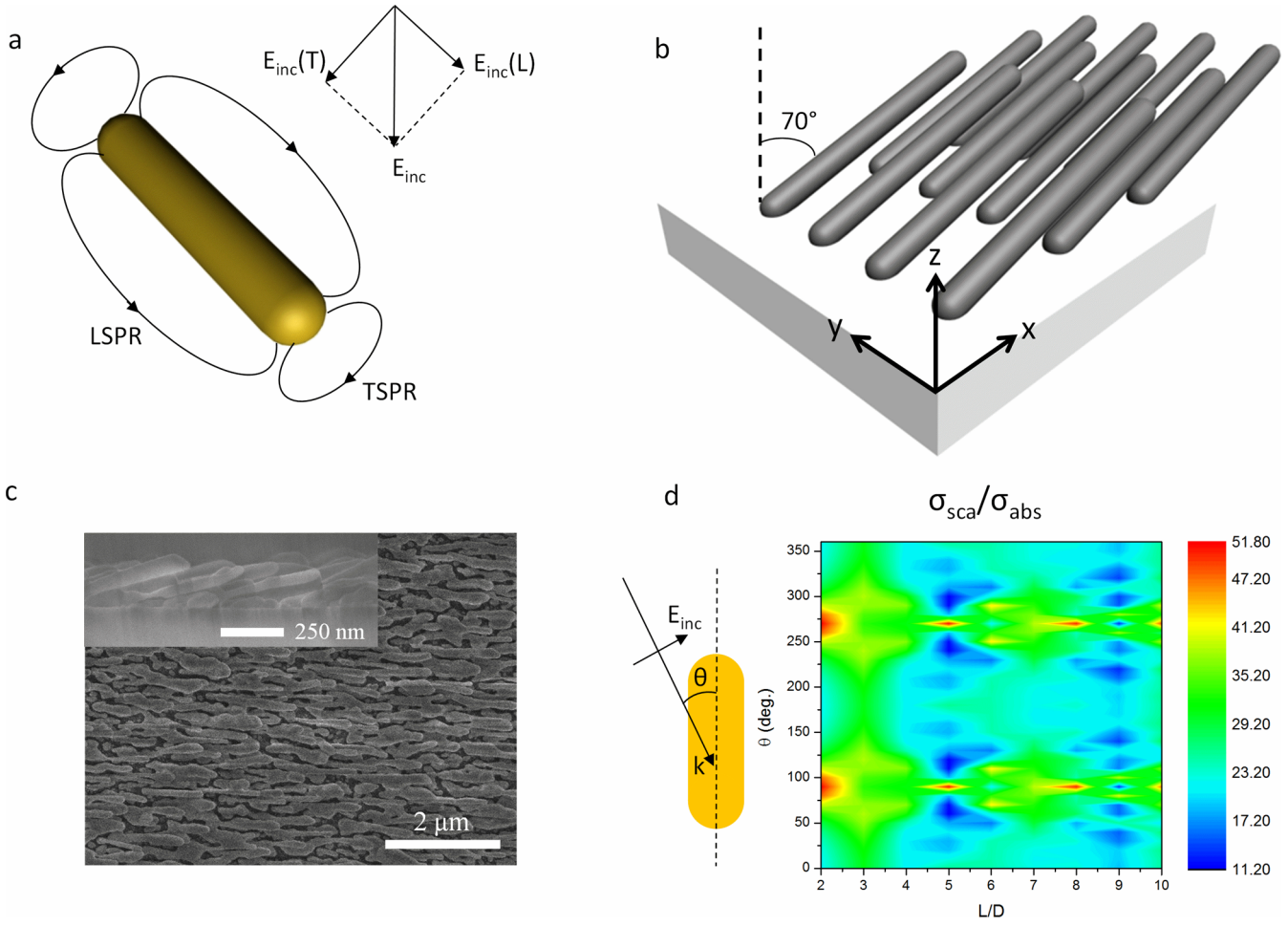

Figure 1. Principle of the plasmonic RL based on metallic NRs and the NR sample. (a) Occurrence of TSPR and LSPR in a metallic NR. The incident light (E_{inc}) is decomposed to the transverse component $E_{inc}(T)$ and longitudinal one $E_{inc}(L)$ so as to excite TSPR and LSPR, respectively. (b) Schematic of slanted silver NRs used for plasmonic RLs. (c) Top-view SEM image of silver NR array sample with L = 917 ± 247 nm and D = 145 ± 39 nm. The inset is a cross-section SEM image of silver NR array. (d) Calculated $\sigma_{sca}/\sigma_{abs}$ as a function of the aspect ratio (L/D) of the NR. In the calculation, the NR diameter is fixed as D = 100 nm and the NR length varies from 200 to 1000 nm. The NR is excited under a p-polarized light at λ = 565 nm.

lasing. It is known that dense metallic nanostructures are detrimental to laser performance due to absorption losses; however, here the lasing threshold keeps decreasing as the metal fraction is increased up to ∼0.07. Spatial-spectral measurements were conducted, revealing the existence of spatially confined lasing modes for the first time in plasmonic RLs. The well-defined orientation of the metallic NRs offers a unique opportunity beyond all-dielectric RLs to manipulate random lasing by directly tuning the polarization of the pump light with respect to the orientation of the metallic NRs. As an illustration of potential applications, we demonstrate that the resultant RLs can serve as miniature bright illumination sources for full-field speckle-free optical imaging of microapertures due to their low spatial coherence.[9] Our results show that the plasmonic RLs can be engineered more compactly than all-dielectric counterparts for such applications.

A metallic NR exhibits an anisotropic plasmonic resonance depending on the properties of the excitation light (e.g., incident angle, polarization), as illustrated in Figure 1a. Typically, two different plasmonic resonances occur in such NRs, one along the short axis of the NR (known as transverse surface plasmon resonance, TSPR) and another along the long axis (longitudinal surface plasmon resonance, LSPR). Controlling light via such an anisotropic response has long been a subject of interest.[30] The optical responses of a metallic NR (e.g., absorption, scattering, and local-field enhancement) depend on the plasmonic resonances. Because these optical properties are vital for controlling RLs, the anisotropic plasmonic resonance behavior may offer a unique way for tuning random lasing. Figure 1b shows the schematic of the silver NR array used for the RLs. The silver NRs are uniformly tilted at an angle roughly 70° from the sample normal. The silver NR array was fabricated with a glancing angle deposition (GLAD) technique (Supporting Information). The dimensions of the NRs were controlled with the deposition time. We have fabricated several samples with the length scales of the NRs ranging from 192 to 917 nm on average (Supporting Information Figure S1). Figure 1c shows a top-view SEM image for the NR array with NR length L = 917 ± 247 nm and diameter D = 145 ± 39 nm. The NR array exhibits a strong scattering signature over a broad wavelength range (Supporting Information Figure S2). The strong scattering capability is beneficial to the formation of highly confined lasing modes, which has been addressed extensively in all-dielectric RLs, but remains undiscovered in plasmonic devices. Because optical absorption and scattering by a metallic nanoparticle contribute

DOI: 10.1021/acs.nanolett.6b00034
Nano Lett. 2016, 16, 2471−2477

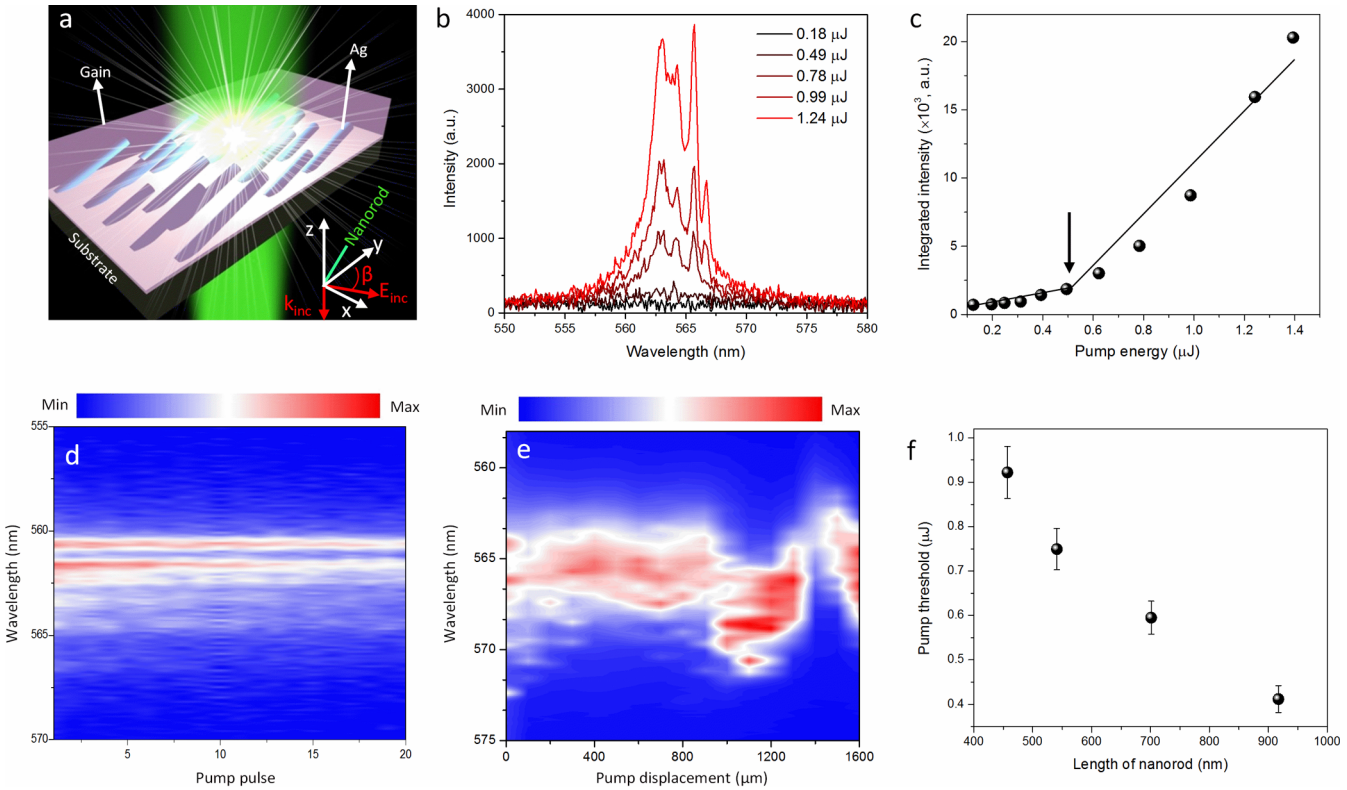

Figure 2. Scheme of the plasmonic RL and random lasing properties. (a) Scheme of the plasmonic RL based on the well-oriented silver NR array. (b) Emission spectra recorded at various pump energies of a picosecond pulsed pump laser (λ = 532 nm). (c) Integrated intensity versus the pump energy. The arrow indicates the pump threshold. (d) Contour map of shot-to-shot lasing spectra obtained upon different pump pulses while keeping the same pump position. (e) Contour map of single-shot lasing spectra obtained upon variation of the pump position. The spectrum was recorded every 100 μm displacement in the pump position. The pump energy for panels d and e is 1.39 μJ. (f) Dependence of the pump threshold on the NR length. The measurements in (b–e) are based on the sample with L = 917 nm. The pump spot size is ~148.0 μm in diameter for (b–f).

oppositely to RLs, we introduce a semiempirical parameter defined as the ratio of the scattering cross section (σ_{sca}) to the absorption one (σ_{abs}) to evaluate the dominance degree of light scattering over absorption. The contour map of $\sigma_{sca}/\sigma_{abs}$ is depicted in Figure 1d, which is calculated on silver NRs with various aspect ratios (L/D) under incidence of a p-polarized wave. The calculation results show that $\sigma_{sca}/\sigma_{abs}$ is larger than 10 everywhere with a large part of the region where $\sigma_{sca}/\sigma_{abs}$ is larger than 20, regardless of the incident angle of the p-polarized light. Further calculations show that $\sigma_{sca}/\sigma_{abs}$ is more profound when the incident wave is s-polarized (Supporting Information Figure S3). The high magnitude of $\sigma_{sca}/\sigma_{abs}$ suggests that these NRs are excellent candidates as light scatterers for highly effective random lasing.[13,18]

To demonstrate a proof-of-concept of the aforementioned plasmonic RLs, we fabricated RLs by covering the 3D silver NR array with a layer of poly(vinyl alcohol) (PVA) film embedded with rhodamine 6G (R6G) molecules (Figure 2a). R6G is an organic laser dye with a high quantum yield and allows for efficient pumping with the second-harmonic output from a Nd:YAG laser (532 nm).[31] The pump laser is directed normal to the sample's surface and a parameter β is introduced to characterize the polarization of the pump light with respect to the orientation of the NRs (Figure 2a). In lasing experiments, the value of β is set as 0°, unless specified otherwise. Figure 2b depicts the evolution of the emission spectrum with the pump energy. At a critical pump energy of ~0.49 μJ, a single sharp peak centered at λ = 563.95 nm emerges over the broad background spectrum with a spectral line width as narrow as 0.20 nm. As the pump energy increases, additional sharp peaks occur and the emission intensity increases more rapidly. The above results are consistent with the behavior exhibited in RLs with coherent feedback:[32] the mode with the highest quality factor will lase first and then the other modes are activated at the higher pumping rate. The pump-dependence of spectrally integrated emission intensity, as plotted in Figure 2c, shows a clear threshold behavior, which further suggests the occurrence of random lasing. Upon multiple shot excitation, the lasing shows photobleaching effects but the frequencies of the lasing peaks are well maintained (Figure 2d), indicating that they are correlated to the existing spatial resonances. On the other hand, the single-shot lasing spectrum varies apparently with the pump position (Figure 2e), suggesting that the lasing modes depend on the local arrangement of NRs. The pump threshold monotonically decreases when L increases from 457 to 917 nm (Figure 2f) because the scattering is stronger for longer nanorods (Supporting Information Figure S2). As the thickness of the gain medium is almost the same in the devices with silver NRs of different length scales, the volume fraction of the metal increases with the NR length (Supporting Information Figure S4). The volume fraction of the metal reaches ~0.07 in the device based on the NR array with L ~ 917 nm, which is at least ~460 times larger than those in existing literature.[13−16,19] For instance, the optimal volume fraction of metallic nanoparticles is ~1.5×10^{-4} in ref 13 (metallic nanoparticle size, D = 55 nm) and ~2.6×10^{-6} in ref 19 (metallic nanoparticle size, D = 12 nm). We suggest that the capability of our RLs working in the presence of such a dense array of metallic NRs can be

DOI: 10.1021/acs.nanolett.6b00034
Nano Lett. 2016, 16, 2471−2477

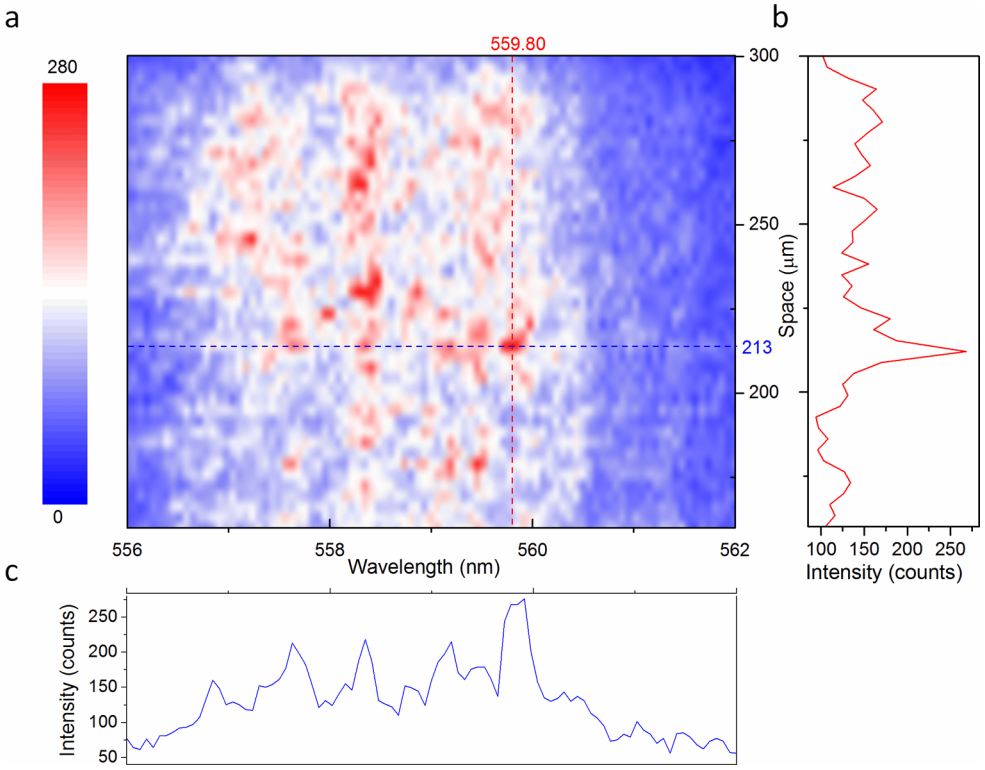

Figure 3. Determine spatial extent of lasing modes via spatial-spectral measurements. (a) Contour map of the spatially resolved lasing spectrum. (b) Spatial profile for the lasing mode centered at λ = 559.8 nm, which is cut along the vertical line in (a). (c) Spectral profile of lasing spatially located at 213 μm, which is cut along the horizontal line in (a). The pump energy is ~10 μJ and the pump spot size is ~300 μm in diameter.

attributed to the fact that the scattering is much stronger than absorption for silver NRs used here (Figure 1d and Supporting Information Figure S3). The metallic nanoparticles used in previous reports typically give much smaller magnitudes of $\sigma_{sca}/\sigma_{abs}$ (Supporting Information Figure S5), which is supposed to account for poor performance of random lasing under a high density of metallic nanoparticles.[13−16,19]

Studies on the spatial confinement of random lasing modes have long been a focus of research,[33−38] especially when the mode size is reduced due to the localization effect.[39] However, so far there are no studies on spatial extents of lasing modes of plasmonic RLs. To investigate the confinement of lasing modes in the NR array, we performed spatial−spectral measurements to determine the spatial extent of random lasing modes (Supporting Information). Figure 3a shows a spatial−spectral image of the emission intensity in a RL device based on silver NRs with L = 541 ± 123 nm pumped above the lasing threshold. Spatially confined lasing modes with mode size at micron scales are clearly observed. Here the mode size is estimated with the full width at half-maximum of the emission intensity profile. Figure 3b corresponds to the spatial profile of the lasing mode centered at λ = 559.80 nm, showing an obvious confinement at ~213 μm with the spatial extent ~5 μm. Figure 3c is the spectral profile for the emission signal spatially projected at ~213 μm, clearly showing spectrally resolved sharp lasing peaks. The resolution of the detection setup is ~5 μm so we are unable to identify smaller spatial features that possibly exist. The above results suggest that the strong scattering capability of the silver NR metamaterial enables mode confinement in RLs.

Previously, controlling random lasing was achieved by engineering the resonance property at the lasing wavelength.[40,41] While effective, this method requires multiple samples with different resonant properties and does not allow tuning of random lasing in a single sample. It was reported that the polarization of the pump light has an impact on random lasing in dielectric systems,[42,43] which is usually related to the spatial profile of the pump light as well as absorption asymmetry of dyes. Here, we demonstrate an approach to tune random lasing in a single device by changing the polarization of the pump laser with respect to the orientation of the NRs (see Figure 2a). In contrast to previous work,[42,43] modulations implemented here truly stems from plasmonic effects of metal, as verified below by comparing to lasing properties enabled by dielectric NRs. As depicted in Figure 4a, the magnitude of the lasing signal is highly dependent on β. We select the most intense lasing mode centered at λ = 564.63 nm and examined the evolution of its intensity with β (Figure 4b). The intensity reaches the maximum when the incident light is polarized at β = 0° or 180° and decreases to the minimum at β = 90°. The intensity recorded under β = 0° is ~3 times higher than that recorded under β = 90°. The lasing emission spectra recorded at β = 0°, 90°, and 180° are compared in Figure 4c. It should be noted the emission spectra recorded at β = 0° and 180° are not the identical to each other but the primary resonant peaks remain. We surmise that the difference arises from a slight photobleaching of dyes upon pumping at a high energy. The pump threshold shows the same trend as the emission intensity upon variation of β, as shown in Figure 4d. We surmise that the profound polarization-dependent lasing behavior might be attributed to the anisotropic scattering properties of the silver NR array. The scattering of the pump light is stronger under β = 0° (Supporting Information Figure S6), which could excite more gain media and lead to stronger

DOI: 10.1021/acs.nanolett.6b00034
Nano Lett. 2016, 16, 2471−2477

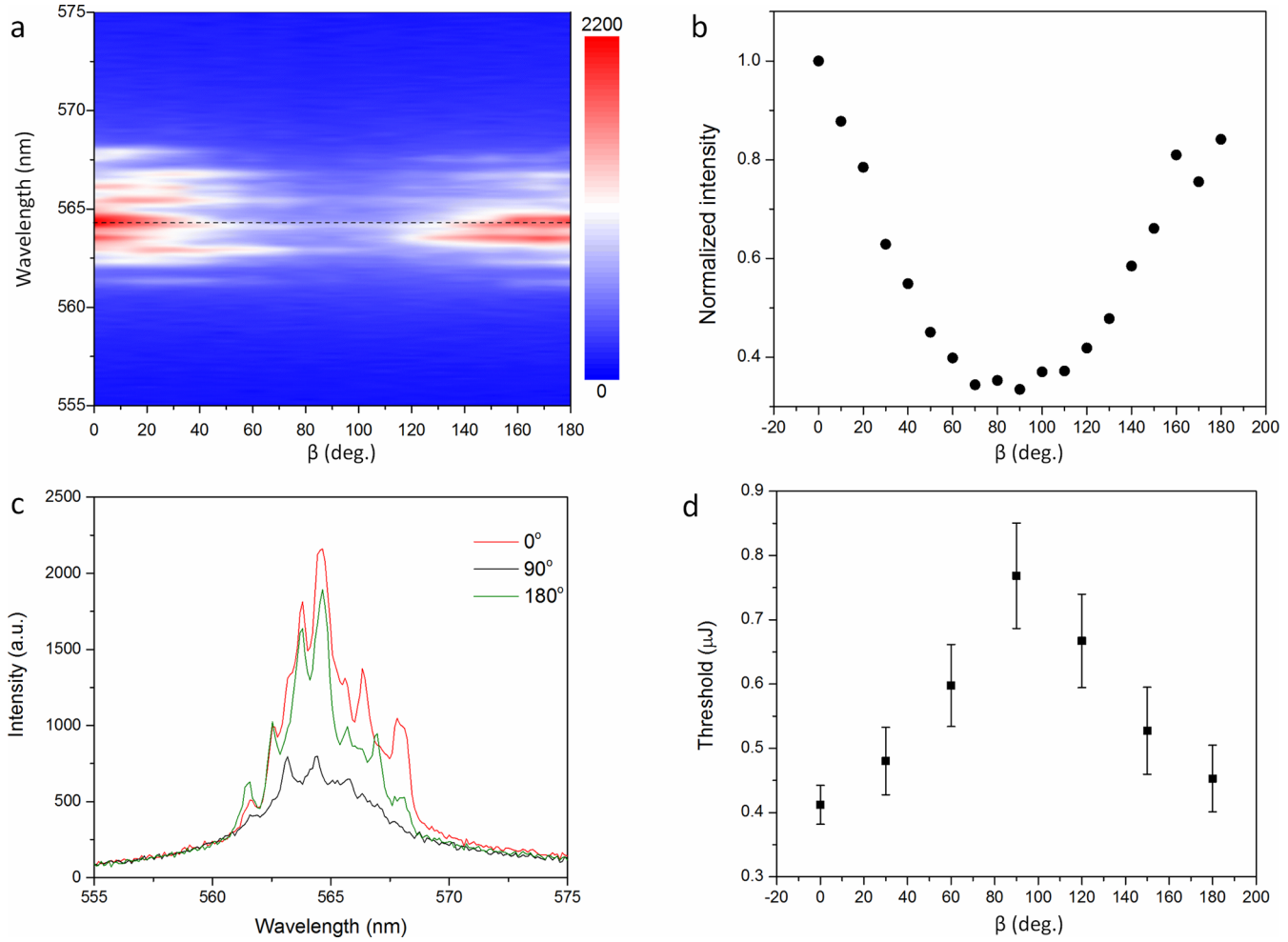

Figure 4. Modulate random lasing by changing the polarization of the pump laser with respect to the orientation of the NRs. (a) Contour map of the lasing spectrum as a function of β. The pump energy is 1.39 μJ and the pump spot size is ~148.0 μm in diameter. (b) β-dependence of the peak intensity for the lasing mode at λ = 564.63 nm (marked with the horizontal dashed line in (a)). The emission intensity was normalized with respect to the maximum one. (c) Emission spectra recorded at β = 0°, 90°, and 180°, respectively. (d) β-dependence of the pump threshold. The sample under study corresponds to the NR array with L = 917 ± 247 nm.

lasing effects. We have examined the other RLs based on NRs with different length scales and observed similar results. For comparison, the emission properties from a RL based on a TiO_2 NR array were examined as well, which have not shown obvious dependence on the pump polarization (Supporting Information Figure S7). Thus, we conclude that the presence of metallic NRs is key to realizing modulation of random lasing. The above results also suggest that the anisotropic plasmonic nanostructures provide more freedom for controlling RLs. This result shows the promise of achieving even stronger modification of random lasing process with metallic nanostructures that are specifically engineered to maximize the anisotropic responses.

A light source with low spatial coherence such as RLs is particularly useful to achieve speckle-free optical imaging because it can prevent the formation of coherent imaging artifacts that generally appear in full-field imaging with conventional lasers as illumination sources.[9] To test the applicability of our RLs to speckle-free imaging, we set up an optical imaging experiment, shown schematically in Figure 5a. A test mark embedded with the "PURDUE" characters in a gold film that has the smallest feature size ~3 μm (Supporting Information Figure S8a) is used as the imaging object (Supporting Information). The RL emission is collected by an objective lens (100×) to illuminate the test mask, and then the resultant image is projected and recorded on a charge-coupled device (CCD) camera. For comparison, the image quality under the illumination of the narrow-band pump laser (λ = 532 nm) is tested by removing the sample and the filter in Figure 5a. As expected, the green pump laser gives a rather poor-quality image showing obvious speckles due to the high spatial coherence of the pump laser (Supporting Information Figure S8b), which is consistent with the existing literature.[9] In contrast, speckle-free images have been obtained when the illumination source is switched to the fabricated plasmonic RLs that are excited under various pump spot sizes (Figure 5b–d). The key to achieving speckle-free imaging is to have many modes lasing simultaneously and independently to suppress the spatial coherence of total emission.[44] As the pump spot size of a RL is reduced, the number of lasing modes decreases correspondingly (Figure 5e–g), which increases the spatial coherence and is thereby detrimental to clear imaging. Therefore, spectral-free imaging is usually achieved under RL illuminations excited beyond a critical pump spot size to have sufficient number of lasing modes. For example, under illumination with all-dielectric RL sources with weak optical

DOI: 10.1021/acs.nanolett.6b00034
Nano Lett. 2016, 16, 2471–2477

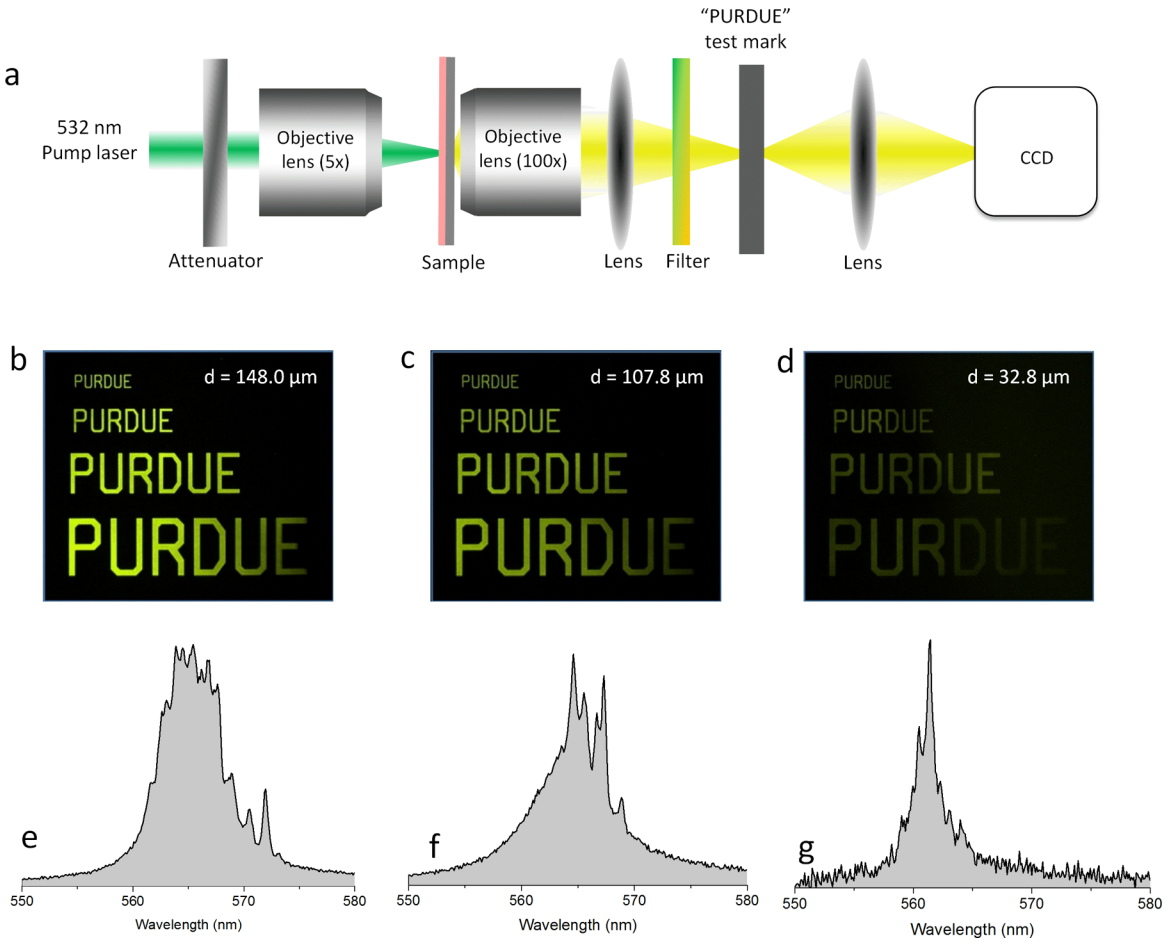

Figure 5. Achieve speckle-free optical imaging with plasmonic RLs as the illumination sources. (a) Optical setup for imaging with plasmonic RLs. A filter is used to filter off the pump light. (b–d) Images of "PURDUE" test mark under the illumination of RLs from the L = 917 nm sample with the pump spot size ~148.0 (b), 107.8 (c), and 32.8 μm (d) in diameter, respectively. The pump spot size is changed by adjusting the position of the objective lens (5×). (e–g) Emission spectra of the RL sources used to illuminate "PURDUE" test mark in (b–d). The pump energy is 1.39 (e,f), and 0.55 μJ (g).

scattering it is difficult to obtain the speckle-free imaging when the pump spot is smaller than 200 μm.[9,45] However, because our plasmonic RL can achieve strong spatial confinement of lasing modes at small scales it is possible to excite enough lasing modes to maintain low spatial coherence even with smaller pump spot sizes. As shown in Figure 5b–d, clear and speckle-free image can be obtained even when the pump spot size is decreased to 32.8 μm, which is ~6-fold smaller than that adopted in all-dielectric RLs.[9,41] This suggests that our RLs can serve as more compact optical sources beyond dielectric counterparts, which could be beneficial to micro- and nanoscale imaging.

To conclude, we presented an approach to achieve highly effective random lasing using 3D plasmonic nanorod metamaterials. First, spatially confined lasing modes at micron scales were observed experimentally. Second, low-threshold lasing was still achieved under a high volume fraction of metal of 0.07. These results imply that one can design random lasers with densely packed metallic nanostructures so as to achieve bright random lasing as long as the metallic nanostructures are carefully engineered. Third, an approach to tune random lasing, which is based on the variation of the polarization of the pump laser, was demonstrated. Such an approach serves as a powerful tool to switch the random lasing in a single device. The demonstrated plasmonic random lasers are well-suited for applications in high-quality optical imaging due to their low spatial coherence. Because plasmonic random lasers herein have the advantage of spatially confined lasing modes at small scales, we were able to achieve speckle-free imaging even when the pump spot size is decreased to 32.8 μm, which is ~6-fold smaller than that in all-dielectric random lasers. The strong scattering capability of the 3D nanorod array is spread over a broad wavelength range; we can thus envision the achievement of tunable, spatially confined, broad-band, and highly compact random lasers with such structures.

■ ASSOCIATED CONTENT

Supporting Information

The Supporting Information is available free of charge on the ACS Publications website at DOI: 10.1021/acs.nanolett.6b00034.

Details on device fabrication, optical measurements, and numerical simulations; SEM images of the silver NR arrays; scattering properties of silver NR arrays with various lengths; calculated $\sigma_{sca}/\sigma_{abs}$ as a function of the aspect ratio of silver nanorods and for a 12 and 55 nm silver sphere used in refs 13 and19; volume fraction of metal in our random laser devices; anisotropic scattering properties of the silver NR metamaterials with L = 917

DOI: 10.1021/acs.nanolett.6b00034
Nano Lett. 2016, 16, 2471–2477

nm; lasing properties of the RL device based on TiO_2 NR array; SEM image of "PURDUE" test mark and its optical image under the illumination of the 532 nm pump laser. (PDF)

AUTHOR INFORMATION

Corresponding Authors

*E-mail: mengxiangeng@gmail.com (X.M.).
*E-mail: aeb@purdue.edu (A.B.).

Author Contributions

X.M., V.M.S., and A.B. designed this work. Z.W. fabricated the samples and made characterizations. Z.W., X.M., S.N., and S.H.C. conducted lasing experiments. Z.W. and X.M. performed numerical simulations. Y.L.K. and H.C. assisted lasing experiments. Z.W. and X.M. wrote the paper and all the other authors commented on the manuscript.

Notes

The authors declare no competing financial interest.

ACKNOWLEDGMENTS

This work is financially supported by Office of Naval Research Grant (MURI N00014-13-0649), Air Force Office of Scientific Research Grant (FA9550-10-1-0264), National Science Foundation Grant (DMR-1120923), and NSF "Meta-PREM" Grant (1205457). The authors acknowledge Dr. Paul West for support in preparation of silver NRs. The authors appreciate Nathaniel Kinsey and Rohith Chandrasekar for proofreading the manuscript and helpful suggestions.

REFERENCES

(1) Letokhov, V. S. *Sov. Phys. JETP* **1968**, *26*, 835−840.
(2) Lawandy, N. M.; Balachandran, R. M.; Gomes, A. S. L.; Sauvain, E. *Nature* **1994**, *368*, 436−438.
(3) Noginov, M. A. *Solid-State Random Lasers*; Springer: Berlin, 2005.
(4) Wiersma, D. S. *Nat. Phys.* **2008**, *4*, 359−367.
(5) Jiang, X. Y.; Soukoulis, C. M. *Phys. Rev. Lett.* **2000**, *85*, 70−73.
(6) Choi, S. H.; Kim, Y. L. *Appl. Phys. Lett.* **2012**, *100*, 041101.
(7) Ma, X. Y.; Chen, P. L.; Li, D. S.; Zhang, Y. Y.; Yang, D. R. *Appl. Phys. Lett.* **2007**, *91*, 251109.
(8) Polson, R. C.; Vardeny, Z. V. *Appl. Phys. Lett.* **2004**, *85*, 1289−1291.
(9) Redding, B.; Choma, M. A.; Cao, H. *Nat. Photonics* **2012**, *6*, 355−359.
(10) Hisch, T.; Liertzer, M.; Pogany, D.; Mintert, F.; Rotter, S. *Phys. Rev. Lett.* **2013**, *111*, 023902.
(11) Leonetti, M.; Conti, C.; Lopez, C. *Nat. Photonics* **2011**, *5*, 615−617.
(12) Bachelard, N.; Gigan, S.; Noblin, X.; Sebbah, P. *Nat. Phys.* **2014**, *10*, 426−431.
(13) Dice, G. D.; Mujumdar, S.; Elezzabi, A. Y. *Appl. Phys. Lett.* **2005**, *86*, 131105.
(14) Popov, O.; Zilbershtein, A.; Davidov, D. *Appl. Phys. Lett.* **2006**, *89*, 191116.
(15) Meng, X. G.; Fujita, K.; Zong, Y. H.; Murai, S.; Tanaka, K. *Appl. Phys. Lett.* **2008**, *92*, 201112.
(16) Meng, X. G.; Fujita, K.; Murai, S.; Tanaka, K. *Phys. Rev. A* **2009**, *79*, 053817.
(17) Zhai, T. R.; Zhang, X. P.; Pang, Z. G.; Su, X. Q.; Liu, H. M.; Feng, S. F.; Wang, L. *Nano Lett.* **2011**, *11*, 4295−4298.
(18) Meng, X. G.; Fujita, K.; Moriguchi, Y.; Zong, Y. H.; Tanaka, K. *Adv. Opt. Mater.* **2013**, *1*, 573−580.
(19) Dominguez, C. T.; Maltez, R. L.; dos Reis, R. M. S.; de Melo, L. S. A.; de Araujo, C. B.; Gomes, A. S. L. *J. Opt. Soc. Am. B* **2011**, *28*, 1118−1123.
(20) Stockman, M. I. *Opt. Express* **2011**, *19*, 22029−22106.
(21) Kelly, K. L.; Coronado, E.; Zhao, L. L.; Schatz, G. C. *J. Phys. Chem. B* **2003**, *107*, 668−677.
(22) Suh, J. Y.; Kim, C. H.; Zhou, W.; Huntington, M. D.; Co, D. T.; Wasielewski, M. R.; Odom, T. W. *Nano Lett.* **2012**, *12*, 5769−5774.
(23) Zhou, W.; Dridi, M.; Suh, J. Y.; Kim, C. H.; Co, D. T.; Wasielewski, M. R.; Schatz, G. C.; Odom, T. W. *Nat. Nanotechnol.* **2013**, *8*, 506−511.
(24) Chen, H. J.; Shao, L.; Li, Q.; Wang, J. F. *Chem. Soc. Rev.* **2013**, *42*, 2679−2724.
(25) Meng, X. G.; Fujita, K.; Murai, S.; Matoba, T.; Tanaka, K. *Nano Lett.* **2011**, *11*, 1374−1378.
(26) Kabashin, A. V.; Evans, P.; Pastkovsky, S.; Hendren, W.; Wurtz, G. A.; Atkinson, R.; Pollard, R.; Podolskiy, V. A.; Zayats, A. V. *Nat. Mater.* **2009**, *8*, 867−871.
(27) Zheludev, N. I.; Prosvirnin, S. L.; Papasimakis, N.; Fedotov, V. A. *Nat. Photonics* **2008**, *2*, 351−354.
(28) Yang, S.; Ni, X. J.; Yin, X. B.; Kante, B.; Zhang, P.; Zhu, J.; Wang, Y.; Zhang, X. *Nat. Nanotechnol.* **2014**, *9*, 1002−1006.
(29) Xiao, S. M.; Drachev, V. P.; Kildishev, A. V.; Ni, X. J.; Chettiar, U. K.; Yuan, H. K.; Shalaev, V. M. *Nature* **2010**, *466*, 735−U6.
(30) Sonnichsen, C.; Franzl, T.; Wilk, T.; von Plessen, G.; Feldmann, J.; Wilson, O.; Mulvaney, P. *Phys. Rev. Lett.* **2002**, *88*, 077402.
(31) Kubin, R. F.; Fletcher, A. N. *J. Lumin.* **1982**, *27*, 455−462.
(32) Cao, H.; Zhao, Y. G.; Ho, S. T.; Seelig, E. W.; Wang, Q. H.; Chang, R. P. H. *Phys. Rev. Lett.* **1999**, *82*, 2278−2281.
(33) Storzer, M.; Gross, P.; Aegerter, C. M.; Maret, G. *Phys. Rev. Lett.* **2006**, *96*, 063904.
(34) Cao, H.; Xu, J. Y.; Zhang, D. Z.; Chang, S. H.; Ho, S. T.; Seelig, E. W.; Liu, X.; Chang, R. P. H. *Phys. Rev. Lett.* **2000**, *84*, 5584−5587.
(35) Anderson, P. W. *Philos. Mag. B* **1985**, *52*, 505−509.
(36) Chabanov, A. A.; Stoytchev, M.; Genack, A. Z. *Nature* **2000**, *404*, 850−853.
(37) Fallert, J.; Dietz, R. J. B.; Sartor, J.; Schneider, D.; Klingshirn, C.; Kalt, H. *Nat. Photonics* **2009**, *3*, 279−282.
(38) van der Molen, K. L.; Tjerkstra, R. W.; Mosk, A. P.; Lagendijk, A. *Phys. Rev. Lett.* **2007**, *98*, 143901.
(39) Segev, M.; Silberberg, Y.; Christodoulides, D. N. *Nat. Photonics* **2013**, *7*, 197−204.
(40) Wu, X. H.; Yamilov, A.; Noh, H.; Cao, H.; Seelig, E. W.; Chang, R. P. H. *J. Opt. Soc. Am. B* **2004**, *21*, 159−167.
(41) Gottardo, S.; Sapienza, R.; Garcia, P. D.; Blanco, A.; Wiersma, D. S.; Lopez, C. *Nat. Photonics* **2008**, *2*, 429−432.
(42) Knitter, S.; Kues, M.; Fallnich, C. *Phys. Rev. A: At., Mol., Opt. Phys.* **2013**, *88*, 013839.
(43) Ito, T.; Tomita, M. *Phys. Rev. E: Stat. Phys., Plasmas, Fluids, Relat. Interdiscip. Top.* **2002**, *66*, 241101.
(44) Schwefel, H. G. L.; Tureci, H. E. *Science* **2015**, *348*, 189−190.
(45) Redding, B.; Choma, M. A.; Cao, H. *Opt. Lett.* **2011**, *36*, 3404−3406.

DOI: 10.1021/acs.nanolett.6b00034
Nano Lett. 2016, 16, 2471−2477